SLAC – PUB – 4340
DPNU – –87 – –23
June 1987
(M)

New Results from the LASS Spectrometer*

D. Aston,[a] N. Awaji,[b] T. Bienz,[a] F. Bird,[a] J. D'Amore,[c] W. Dunwoodie,[a] R. Endorf,[c] K. Fujii,[b‡] H. Hayashii,[b§] S. Iwata,[b] W.B. Johnson,[a] R. Kajikawa,[b] P. Kunz,[a] D.W.G.S. Leith,[a] L. Levinson,[a♮] T. Matsui,[b‡] B.T. Meadows,[c] A. Miyamoto,[b‡] M. Nussbaum,[c] H. Ozaki,[b] C.O. Pak,[b‡] B.N. Ratcliff,[a] D. Schultz,[a] S. Shapiro,[a] T. Shimomura,[b] P. K. Sinervo,[a†] A. Sugiyama,[b] S. Suzuki,[b] G. Tarnopolsky,[a♯] T. Tauchi,[b‡] N. Toge,[a] K. Ukai,[d] A. Waite,[a♮♮] S. Williams[a♯♯]

[a] *Stanford Linear Accelerator Center, Stanford University, P.O. Box 4349, Stanford, California 94305, U.S.A.*
[b] *Department of Physics, Nagoya University, Furo-cho, Chikusa-ku, Nagoya 464, Japan*
[c] *University of Cincinnati, Cincinnati, Ohio 45221, U.S.A.*
[d] *Institute for Nuclear Study, University of Tokyo, Midori-cho, Tanashi, Tokyo 188, Japan*

ABSTRACT

New results are presented from analyses of several mesonic and baryonic states containing one or more strange quark. The data are taken from a high statistics (4 events/nb) study of K^-p interactions at 11 GeV/c carried out in the LASS Spectrometer at SLAC. New information is reported on the underlying K^* states and also evidence for selective coupling of $K^-\eta$ to the K^*'s; on the strangeonium members of the axial vector nonets in the $K\overline{K}\pi$ channel; and on evidence for an Ω^{*-} state.

Talk presented by S. Suzuki at the 2nd International Conference on Hadron Spectroscopy, KEK, Tsukuba, Japan April 16-18, 1987

* Work supported in part by the Department of Energy under contract No. DE-AC03-76SF00515; the National Science Foundation under grant Nos. PHY82-09144, PHY85-13808, and the Japan U.S. Cooperative Research Project on High Energy Physics.

‡ Present Address: National Laboratory for High Energy Physics, KEK, Oho-machi, Tsukuba, Ibaraki 305, Japan.
§ Present Address: Nara Women's University, Kitauoya-nishi-machi, Nara 630, Japan.
♮ Present Address: Weismann Institute, Rehovot 76100, Israel.
† Present Address: University of Pennsylvania, Philadelphia, Pennsylvania 19104, U.S.A.
♯ Present Address: Hewlett-Packard Laboratories, 1501 Page Mill Road, Palo Alto, California 94304, U.S.A.
♮♮ Present Address: Dept. of Physics, University of Victoria, Victoria BC, Canada V8W 2Y2
♯♯ Present Address: Diasonics Corp., 533 Cabot Rd., S. San Francisco, CA 94090, U.S.A.

1. Overview and Introduction

Several candidates have been reported for glueballs and exotic mesons in various experiments[1] . Most of these states lie in the 1.0 – 2.5 GeV/c^2 mass region, and they are easily confused with conventional $q\bar{q}$ states. To help settle the nature of these candidates, it is very important to make a full map of $q\bar{q}$ mesonic states, exploring the spectrum of excitations, as well as to search for exotic states which are directly produced in the hadronic processes. Since light quark spectroscopy has been studied for a long time, an experiment is required to have both high sensitivity and good acceptance in a wide variety of physics channels to make significant progress. The report here describes an effort towards addressing these issues in an experiment utilizing the Large Aperture Superconducting Solenoid (LASS) spectrometer at SLAC.

A schematic view of the LASS spectrometer is shown in fig. 1. This spectrometer is characterized by a clean RF separated K^- beam, flat acceptance over nearly 4π steradians, and a bias free trigger for events with $\geq$2 charged particles as defined in the planar and cylindrical proportional chambers surrounding the target. Two threshold Čerenkov counters, a time of flight counter hodoscope, and dE/dx measurement in the cylindrical proportional chambers around the target provide good particle identification. The details of the spectrometer are described elsewhere[2] .

We accumulated 113 million K^-p events, corresponding to a sensitivity of 4.1 events/nb. The results presented below come from the study of strange mesons in the $K^-\pi^+$ and $K^-\eta$ channels, strangeonium mesons in the $K\overline{K}\pi$ and $K\overline{K}$ channels, and the strangeness -3 baryons in the $\Xi^{*0}(1530)K^-$ channel. As some of these results have already been presented[3] at the Berkeley conference, we concentrate on progress since then, especially on a study of underlying K^* states in the $K^-\pi^+$ channel; a check of SU(3) in the $K\eta$ coupling to the K^*'s; an $s\bar{s}$ axial vector search in the $K\overline{K}\pi$ channel which is important with respect to the E/ι puzzle; and a search for Ω^{*-} states.

2. Strange Mesons

2.1 $K^-\pi^+$ SCATTERING

The simple topology and large cross section of the $K^-\pi^+$ final state provide an ideal place for studying natural J^{PC} states. The leading orbitally excited states of the K^* resonances were explored up through $J^P = 5^-$ by the spherical harmonic moments method, and the results have already been published[4] . These moments and information from a t-dependent parametrization of the production amplitude have been used to perform an energy independent partial wave analysis of the $K^-\pi^+$ system from threshold to 2.6 GeV/c^2, for the purpose of studying $K^-\pi^+$ two body scattering.

Fig. 2 shows the results of the partial wave analysis. The amplitudes are uniquely determined up to 1.84 GeV/c^2, and there is essentially a two fold ambiguity only in the non-leading waves above 1.84 GeV/c^2 as shown by solutions A and B in fig. 2. In either case, the amplitudes corroborate the leading L-excited states ($K^*(892)$, $K_2^*(1430)$, $K_3^*(1780)$, $K_4^*(2060)$ and $K_5^*(2380)$) directly observed in the moments, and also provide new evidence for the underlying states in S and P waves.

The low mass 0^+ amplitude shown in figs. 3(a) and (b) confirms the $K_0^*(1350)$ [was κ] observed by earlier experiments. The lines on the figure are the results of a fit to the model of P. Estabrooks et al[5] which gives parameter values for the mass and width of M = 1429 $\pm$ 4 $\pm$ 5 MeV/c^2 and Γ = 287 $\pm$ 10 $\pm$ 21 MeV/c^2, respectively. However, other models give values which differ from these by up to 100 MeV/c^2. Figs. 3(c) and (d) also show evidence for a second 0^+ $K_0^*(1950)$ at higher mass in both solutions A and B, with M = 1934 $\pm$ 8 $\pm$ 20 MeV/c^2, Γ = 174 $\pm$ 19 $\pm$ 79 MeV/c^2 for solution A, and M = 1955 $\pm$ 10 $\pm$ 8 MeV/c^2, Γ = 228 $\pm$ 34 $\pm$ 22 MeV/c^2 for solution B, respectively.

Fig. 4 shows the P wave amplitude in the region of no ambiguity. In addition to the well known $K^*(892)$, the amplitude displays clear resonant structure around 1740 MeV/c^2, which confirms the $K^*(1790)$. However, these two resonances plus background do not give a good fit to the amplitude in the region around 1400 MeV/c^2 as shown by the dashed line in fig. 4. When an additional resonance is added, the model shown by the solid curve fits the data very well. The values obtained for the two higher mass resonances are M = 1380 $\pm$ 21 $\pm$ 19 MeV/c^2, Γ = 176 $\pm$ 52 $\pm$ 22 MeV/c^2 for the $K^*(1410)$, and M = 1677 $\pm$ 10 $\pm$ 32 MeV/c^2, Γ = 205 $\pm$ 16 $\pm$ 34 MeV/c^2 for the

$K^*(1790)$. Both of these states have been observed in the $K^0\pi^+\pi^-$ three body PWA, but this is the first observation of the $K^*(1410)$ decaying into $K\pi$. The small coupling to the $K\pi$ mode could be a direct consequence of a node in the radial wave function, which gave small overlapping integral in the two body decay amplitude[6] .

As a summary, fig. 5 shows the list of K^* states observed in the $K^-\pi^+$ channel.

2.2 $K^-\eta$ CHANNEL

In contrast to the extensive study of K^*'s in the $K\pi$ and $K\pi\pi$ channels, no serious attempt to look for these states in the $K\eta$ channel in a high statistics experiment has been made so far. The $K^* \to K\eta$ branching ratio can be calculated in SU(3), hence comparing these ratios with $K^* \to K\pi$ provides us a good check of SU(3) symmetry with a new channel.

The reaction $K^-p \to K^-\pi^+\pi^-\pi^0 p$ is selected by a 1C fit, and exhibits a clear η signal in the $\pi^+\pi^-\pi^0$ mass spectrum (fig. 6). Selecting the η region, the $K^-\eta$ effective mass spectrum shows a prominent peak around 1.75 GeV/c^2 (fig. 7). A background subtracted spherical moments analysis and subsequent amplitude decomposition shows this peak is dominated by $J^P = 3^-$ (fig. 8(a)). A Breit-Wigner fit to the preliminary F wave amplitude gives M = 1749 $\pm$ 10 MeV/c^2, and Γ = 193 $\pm$ 43 MeV/c^2, with systematic errors still to be determined. The peak is most naturally interpreted as $K_3^*(1780)$. Using the $K\pi$ data of the CERN-Geneva group[8] , the relative width of $K\eta$ to $K\pi$ is

$$R_3 = \frac{\Gamma(K_3^*(1780) \to K\eta)}{\Gamma(K_3^*(1780) \to K\pi)} = 0.54 \pm 0.22.$$

If we assume the PDG value[7] for $BR(K^*(1780) \to K\pi) = 17 \pm 5\%$, we get $BR(K_3^*(1780) \to K\eta) = 9.2 \pm 4.4\%$.

On the other hand, no positive evidence for $K_2^*(1430)$ is observed in either the $K^-\eta$ mass spectrum or the D wave amplitude (fig. 8(b)). The upper limit of the relative widths of $K\eta$ to $K\pi$ for the $K_2^*(1430)$ is estimated to be

$$R_2 = \frac{\Gamma(K_2^*(1430) \to K\eta)}{\Gamma(K_2^*(1430) \to K\pi)} < 0.91\ \%$$

at the 95% confidence level, which leads to a limit on the $K\eta$ branching ratio $BR(K_2^*(1430) \to K\eta)$ of 0.41% at the 95% confidence level. The PDG quoted value[7] of 5.2 $\pm$ 2.9 % is far from our measurement.

The dramatic difference between the $K\eta$ coupling to $K_2^*(1430)$ and to $K_3^*(1780)$ (R_2 and R_3) looks odd. However, it is explained by an SU(3) model with octet-singlet mixing of the η and η'. The main difference comes from the D and F type meson couplings, according to the symmetry of the parent and daughter states. A straightforward calculation gives

$$R_2 = \frac{\Gamma(K_2^*(1430) \to K\eta)}{\Gamma(K_2^*(1430) \to K\pi)} = \frac{1}{9}(cos\theta_p + 2\sqrt{2}sin\theta_p)^2 \left(\frac{q_{K\eta}}{q_{K\pi}}\right)^5,$$

and

$$R_3 = \frac{\Gamma(K_3^*(1780) \to K\eta)}{\Gamma(K_3^*(1780) \to K\pi)} = (cos\theta_p)^2 \left(\frac{q_{K\eta}}{q_{K\pi}}\right)^7,$$

where $q_{K\eta}$ and $q_{K\pi}$ are the c.m. momenta of the final $K\eta$ and $K\pi$ states, respectively, and θ_p is the SU(3) octet-singlet mixing angle of the η and η' in the 0^- nonet. R_2 has a suppression factor of 9 compared to the R_3, and has a further suppression from the negative mixing angle θ_p, while R_3 is rather insensitive to θ_p. For example,

$\theta_p = 0.0° : R_2 = 3.2\%, R_3 = 41\%$

$\theta_p = -10.0° : R_2 = 0.8\%, R_3 = 40\%$

$\theta_p = -18.5° : R_2 = 0.0\%, R_3 = 37\%$

$\theta_p = -23.0° : R_2 = 0.1\%, R_3 = 34\%$

The data are roughly consistent with today's generally accepted θ_p value ($-10° < \theta_p < -23°$). The flux tube model calculation by Kokoski and Isgur[9] also gives very similar values to those of the above naive SU(3) model [$R(K_2^*(1430)) \sim 1\%$ and $R(K_3^*(1780)) \sim 50\%$], basically in agreement with our results.

3. Strangeonium

K^-p hypercharge exchange processes with backward going Λ's are expected to be a rich source of $s\bar{s}$ states. Below are some results of analyses of exclusive processes with Λ vertices reconstructed in the spectrometer. Hence, rather loose requirements on the particle identifying devices provide very clean identification of these processes with uniform acceptance.

3.1 $K\overline{K}\pi$ CHANNEL

Mesons decaying to $K\overline{K}\pi$ are studied in the $K^-p \to K^0_s K^\pm \pi^\mp \Lambda$ exclusive channels. The most important issues are to determine the $s\bar{s}$ members of 1^+ nonets. Defining these states will play an important role in sorting out the E/ι puzzle.

Fig. 9 shows the effective mass spectrum of $K^0_s K^\pm \pi^\mp$ with $K^0_s K^+ \pi^-$ and $K^0_s K^- \pi^+$ combined. The spectrum is characterized by a rapid rise at the $K^*\overline{K}$ + c.c. threshold, and peak structures around 1.5 and 1.9 GeV/c^2. There is no clear evidence for significant production of an '$E(1420)$' in contrast with expectations if its quark content is dominantly $s\bar{s}$.

We carried out an isobar model three body partial wave analysis using these data. The threshold region and the first peak after the $K^*\overline{K}$ + c.c. threshold are seen in fig. 10 to be mostly 1^+ while the second peak around 1.9 GeV/c^2 is associated mainly with 2^- and some 3^- waves. There are no prominent structures in the 0^-, 1^- and 2^+ waves.

Checking the dominant 1^+ wave in more detail, we see that the production of the K^* and $\overline{K}^*$ are asymmetric in the region below 1.6 GeV/c^2 (fig. 11). This is also clear from the Dalitz plot (not shown). It is hard to explain such an asymmetry if a single $s\bar{s}$ resonance contributes. This motivates us to check the interference of the $K^*\overline{K}$ and $\overline{K}^*K$ waves. The interference pattern shows interesting features. Namely, it is negative right after the $K^*\overline{K}$ + c.c. threshold and then becomes positive at 1.5 GeV/c^2 (fig. 12). Since opposite G-parity states interfere with opposite signs, this indicates the existence of at least two objects with opposite G-parity in this mass region.

As the $K^*\overline{K}$ and $\overline{K}^*K$ waves themselves are not G-parity eigenstates, the amplitudes are decomposed into the G-eigenstates J^{PG}, and the 1^+ waves split into 1^{++} and 1^{+-} waves (fig. 13). Note that for isospin zero objects, J^{PG} coincides with J^{PC}. With this assumption the $J^{PC} = 1^{++}$ amplitude has a clear peak at 1.53 GeV/c^2 with $\Gamma \sim 80$ MeV/c^2. This observation is in good agreement with the $D'(1530)$ reported by Gavillet et al[10] , and since it is strongly produced in K^-p hypercharge exchange reaction, it is an excellent candidate for the $s\bar{s}$ member of the 1^{++} nonet. The 1^{+-} wave is strongly peaked towards the $K^*\overline{K}$ + c.c. threshold and provides a good candidate for the $s\bar{s}$ member of the 1^{+-} nonet. Because of the proximity of the $K^*\overline{K}$ + c.c. threshold, it's mass and width are somewhat difficult to determine, but they lie within the range $1.3 < M < 1.45$ GeV/c^2 and $\Gamma < 150$ MeV/c^2.

In summary, there is no sharp $E(1420)$ signal in the K^-p hypercharge reaction, suggesting that the $E(1420)$ is not dominantly an $s\bar{s}$ object. Instead, a 1^{++} $f_1'(1530)$ $[D'(1530)]$ exists as an $s\bar{s}$ candidate member of the 1^{++} nonet, and evidence for a 1^{+-} $h'(1380)$ $[H']$ is also seen. These two states fit rather well into nonets, where the 1^{++} nonet includes the $a_1(1270)$, $K_{1A}(1340)$, $f_1(1285)$ and $f_1'(1530)$, while the 1^{+-} nonet contains the $b_1(1235)$, $K_{1B}(1340)$, $h_1(1190)$ and $h'(1380)$.

3.2 $K\overline{K}$ CHANNEL

The exclusive reactions $K^-p \rightarrow K^+K^-\Lambda$ and $K_s^0K_s^0\Lambda$ have also been analyzed. These reactions provide new information on the $s\bar{s}$ leading L-excited states, and also permit interesting comparisons with the $K\overline{K}$ spectrum produced in "glue enriched" channel of radiative J/ψ decay.

In fig. 14 the raw K^+K^- mass spectrum is shown. The K^+K^- channel suffers from strong diffractive production of N^*'s in the $K^+\Lambda$ channel. The mass spectrum with the requirement of $M_{K^+\Lambda} > 2.0$ GeV/c^2 is shown by the shaded histogram. In both spectra, we can see a strong $\phi(1020)$ peak, a clear $f_2'(1525)$ $[f']$ peak, and evidence for a $\phi_3(1860)$. On the other hand, $K_s^0K_s^0$ is relatively background free, and only couples to even spin objects due to Bose statistics. The acceptance corrected $K_s^0K_s^0$ mass spectrum is shown in fig. 15. The only strong peak seen is the $f_2'(1525)$. In either case, the $f_2(1720)$ $[\theta]$ is not seen, suggesting that the $f_2(1720)$ $[\theta]$ is unlikely to be a conventional $s\bar{s}$ meson.

A previous spherical moments analysis of the K^+K^- channel has reported structure at 1.86 GeV/c^2 in the corrected mass distribution (t_{00}) and the higher moments up to t_{60}[8] , suggesting the spin parity of the peak at 1.86 GeV/c^2 is 3^-. This has been confirmed by an amplitude analysis. Fig. 16 shows a preliminary result of the subsequent amplitude decomposition for the F-wave. A Breit-Wigner fit to the amplitude gives the resonance parameters M = 1859 $\pm$ 17 MeV/c^2 and Γ = 144 $\pm$ 55 MeV/c^2.

Below 2.0 GeV/c^2, the acceptance corrected $K_s^0K_s^0$ mass distribution (fig. 15) is well fit by a sum of the $f_2(1270)$ $[f]$ and $f_2'(1525)$ $[f']$ resonances without the $f_2(1720)$ $[\theta]$. The resonance parameters are consistent with other data, and the upper limit of the $f_2(1720)$ $[\theta]$ production cross section times its branching ratio to the $K_s^0K_s^0$ channel is 91 nb at the 95 % confidence level.

There are some excess events clustered right above the $K_s^0 K_s^0$ threshold. Though these events may be considered to result from decays of either the conventional $f_0(975)$ [S] or the $a_0(980)$ [δ], the narrowness of the structure leads to some preference for a narrower object closer to the $K\overline{K}$ threshold. Such an object (the $S_2(988)$) has been suggested by Au, Morgan and Pennington[11] in a recent analysis of several different channels including new data from CERN ISR. Their analysis also suggests at least one additional resonance in the same mass region which is proposed as a good candidate for the lightest glueball.

Some structure exists where MARK III claimed the existence of $X(2200)$ [ξ]. Fig. 17(b) shows the comparison of the effective mass distributions from LASS and MARK III in the 2.2 GeV/c^2 region. The mass spectra are very similar with a small structure on top of a broad enhancement. The decay angular distribution of our events peak forward (backward) (fig. 17(a)), and the data also show t_{20} and t_{40} moments are associated with this structure, indicating the spin J of this peak to be $J \geq 2$.

4. Search for Ω^*.

Finally, we briefly report on a search for Ω^*s. From the events with a V$^-$ topology, we select the $\Xi^-\pi^+K^-$ candidate sample requiring K^- identification by the Čerenkov counters. After selecting events where the $\Xi^-\pi^+$ combination results from the decay of a $\Xi^{*0}(1530)$, clean evidence appears for a Ω^{*-} peak around 2.26 GeV/c^2 (fig. 18(a)). This figure also includes estimates for the non-$\Xi^{*0}(1530)$ background and π^- punch-through due to finite efficiency of the Čerenkov counters. The peak does not result from misidentified π's as can be seen by taking positively identified π^-'s as K^-'s which have the same momentum space and not seeing any structure (fig. 18(b)). A Breit-Wigner fit to the background subtracted $\Xi^{*0}K^-$ mass spectrum (fig. 19) shows the parameters to be M = 2253 $\pm$ 13 MeV/c^2 and Γ = 77 $\pm$ 35 MeV/c^2. The signal is estimated to contain 48 $\pm$ 12 events, corresponding to an inclusive cross section of 630 $\pm$ 180 nb.

It would be interesting to compare this state with the states reported by the CERN hyperon beam group[12] , as well as the levels several theoretical models predict[13] . Unfortunately, spin-parity information is not available from either of the experiments due to the limited acceptance of the particle identification devices, so this question remains a matter of speculation at this moment.

5.-Summary and Conclusions

We have obtained a good scope on the details of $q\bar{q}$ spectroscopy, and have states ranging over 5 units of orbital excitations and 2 units of radial excitation quantum numbers. The $q\bar{q}$ states discussed in this report are summarized in fig. 20. We now have good candidates for almost all the $q\bar{q}$ structure expected in K^*s below 2.0 GeV/c^2 and see the orbitally excited states extending to higher mass. Many of the structures expected in the strangeonium spectrum are seen as well. The $K\eta$ final state shows selective coupling to different K^*'s, implying that SU(3) is still able to predict interesting features of the meson spectrum. The long and confusing story of the $s\bar{s}$ axial vector nonets around 1.4 - 1.5 GeV/c^2 has become much clearer since this experiment, containing an s-quark in the beam, gives evidence that the $f_1'(1530)$ [$D'(1530)$] and $h'(1380)$ [H'] are the $s\bar{s}$ members of the 1^{++} and 1^{+-} nonets. Finally, we have good evidence for the production of an excited strangeness = -3 baryon (Ω^*) at 2253 MeV/c^2.

REFERENCES

1. C. Edwards et al., Phys. Rev. Lett. 48 (1982) 458
   A. Etkin et al., Phys. Rev. Lett. 49 (1982) 1620
   D. M. Coffman et al., SLAC-PUB 3720 (1986)
   R. M. Baltrusaits et al., Phys. Rev. Lett. 56 (1986) 107
   D. Alde et al., Nucl. Phys. B269 (1986) 485
2. D. Aston et al., The LASS Spectrometer, SLAC-REP-298, May 1986.
3. D. Aston et al., SLAC-PUB-4054/DPNU-86-46
4. D. Aston et al., Phys. Lett. 180B (1986) 308
5. P. Estabrooks et al., Nucl. Phys. B133 (1978) 490
6. A. Bradley, J. Phys., G4 (1978) 1517
   E. Eichten et al., Phys. Rev. D21 (1980) 203
   S. B. Gerasimov et al., Z. Phys. C13 (1982) 43
7. Review of Particle Properties, Particle Data Group, Phys. Lett. 170B (1986) 1
8. W. E. Cleland et al., Nucl. Phys. B208 (1982) 189
   R. Baldi et al., Phys. Lett. 63B (1976) 344
9. R. Kokoski and N. Isgur, preprint UTPT-85-05
10. P. Gavillet et al., Z. Phys. C16 (1982) 119
11. K. L. Au, D. Morgan and M. R. Pennington, RAL 86-76
12. S. F. Biagi et al., Z. Phys. C31 (1986) 33
13. For example, N. Isgur and G. Karl, Phys. Rev. D19 (1979) 2653

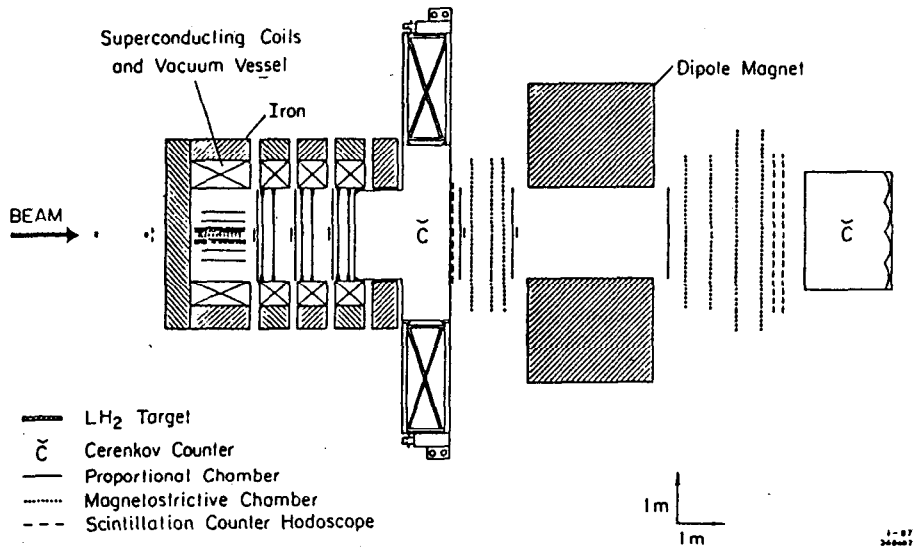

Fig. 1. Schematic drawing of the LASS spectrometer.

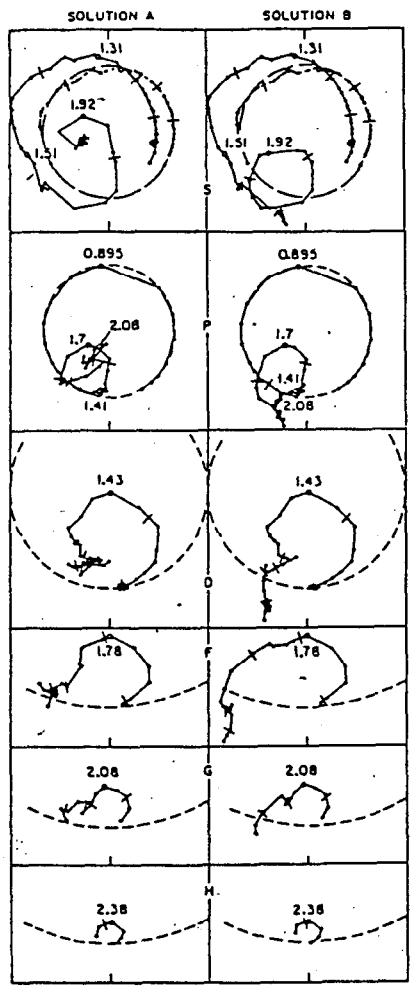

Fig. 2. Argand diagram of $K^-\pi^+$ scattering amplitude.

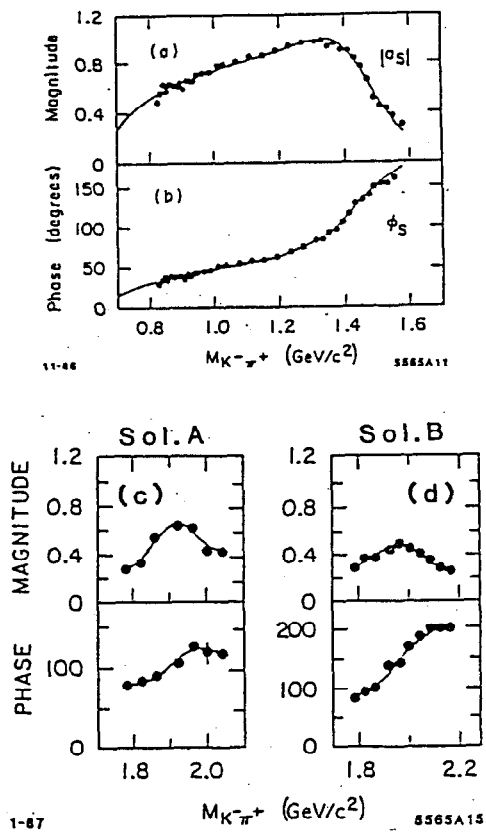

Fig. 3. $K^-\pi^+$ S-wave amplitude.

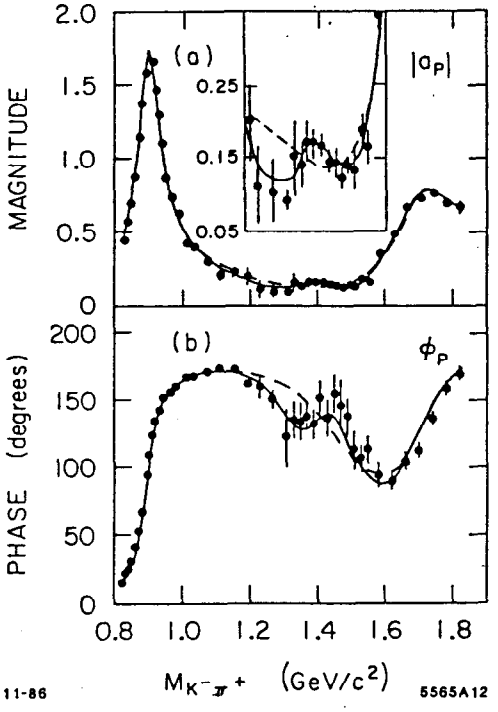

Fig.4. $K^-\pi^+$ P-wave amplitude.

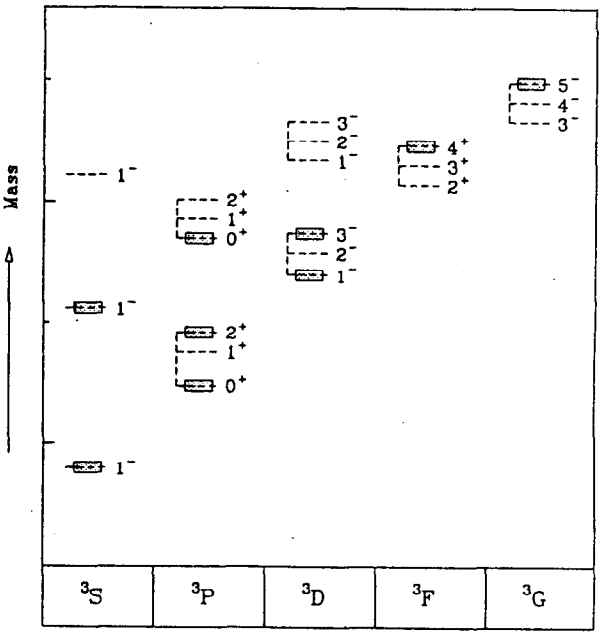

Fig.5. Summary of K^* states observed in the $K^-\pi^+$ two body analysis.

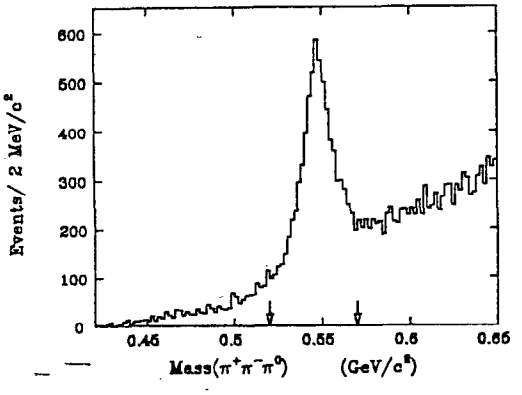

Fig.6. Effective mass spectrum of $\pi^+\pi^-\pi^0$ in the $K^-p \to K^-\pi^+\pi^-\pi^0 p$ process showing the η region used in the analysis.

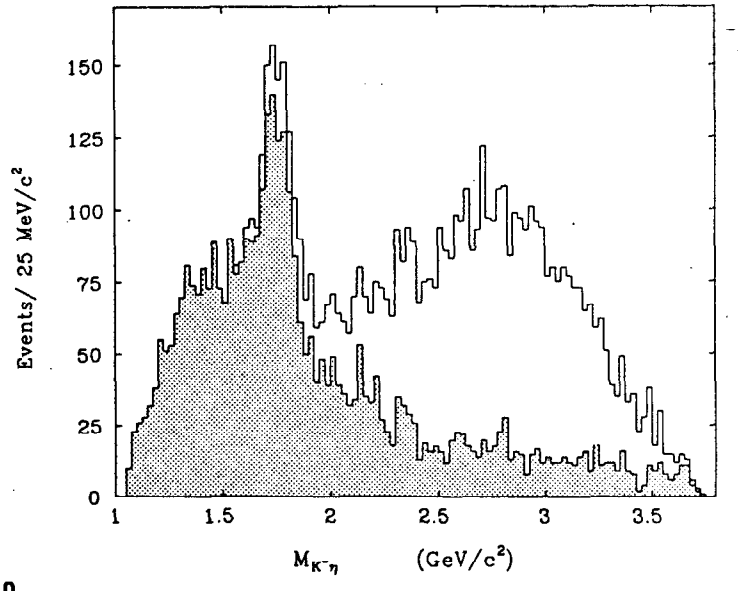

Fig.7. Effective mass distribution of $K^-\eta$. Shaded histogram shows the results after the diffractive backgrounds are removed by the requirement of $M_{\eta p} > 2.0$ GeV/c² and $M_{K^-p} > 1.85$ GeV/c².

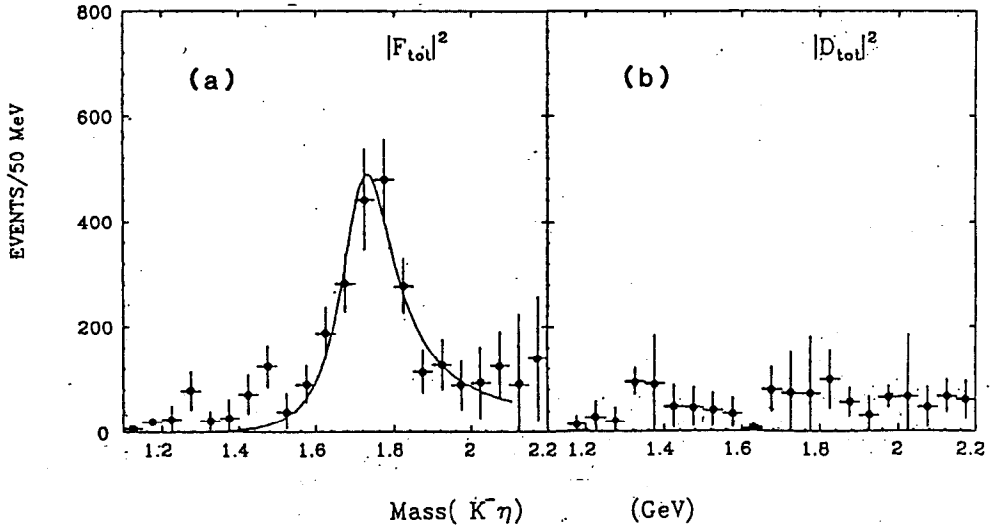

Fig. 8. Intensity of the (a) F and (b) D wave amplitudes in the $K^-\eta$ channel. A Breit-Wigner fit to the dominant F-wave is superposed.

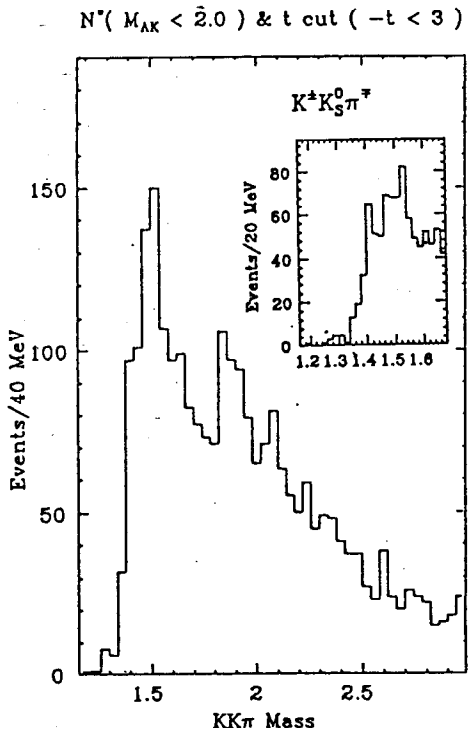

Fig. 9. Effective mass spectrum of $K^0_s K^\pm \pi^\mp$, with the $K^0_s K^+ \pi^-$ and $K^0_s K^- \pi^+$ final states combined. Inlet shows the plot with finer mass bins.

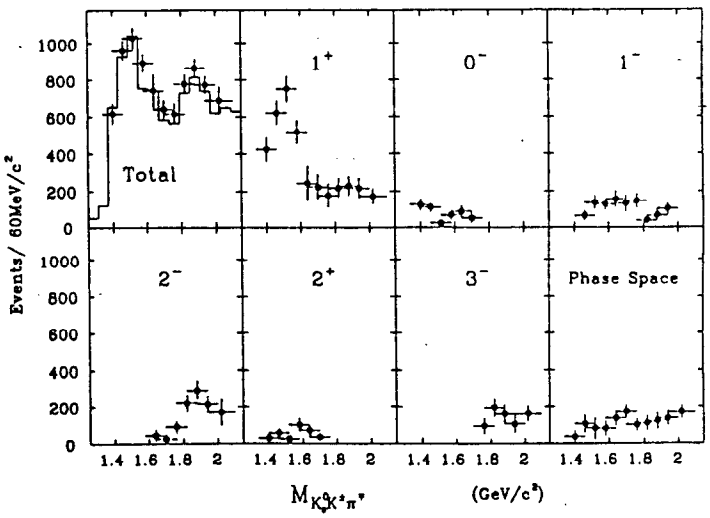

Fig. 10. J^P decomposition of $K^0_s K^\pm \pi^\mp$ waves.

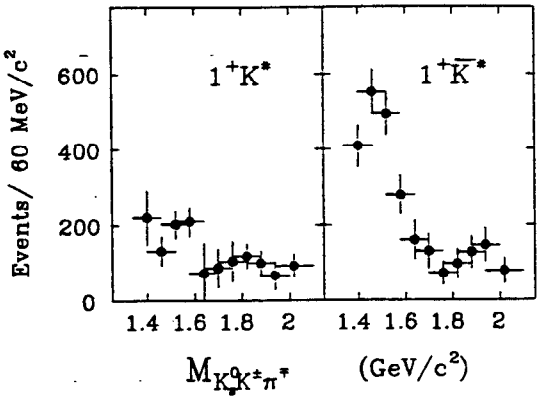

Fig.11. Breakdown of the 1^+ wave into $K^*\overline{K}$ and $\overline{K}^*K$ components.

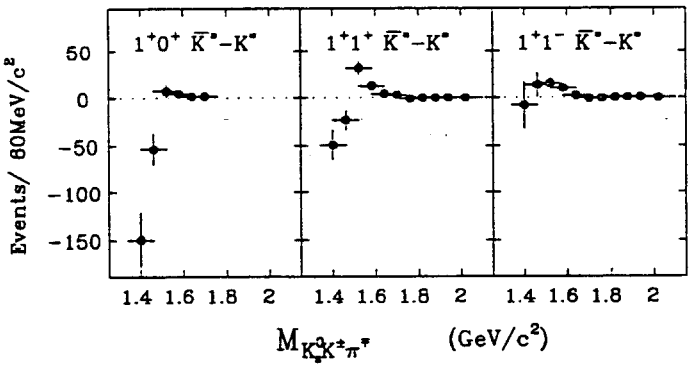

Fig.12. Mass dependence of $K^*\overline{K}$ - $\overline{K}^*K$ interference.

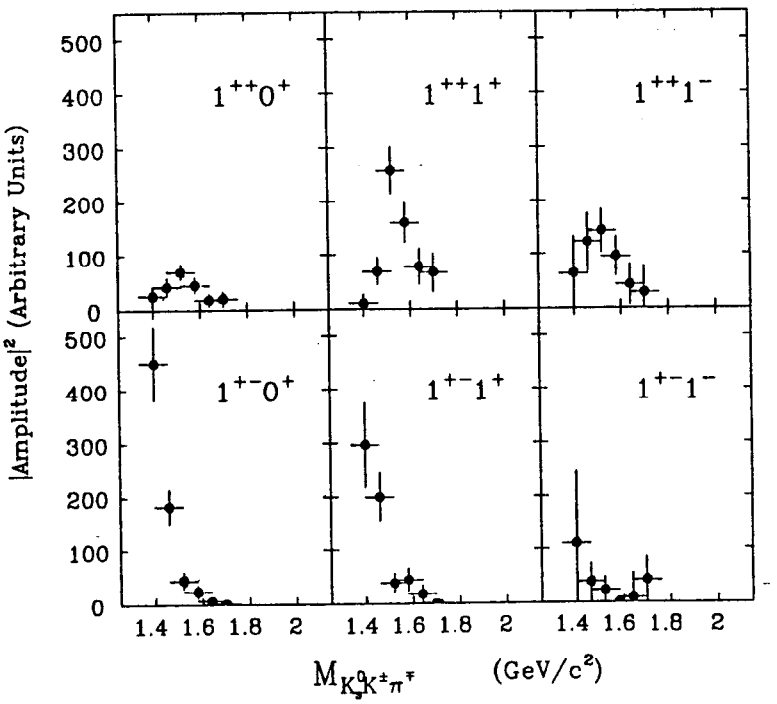

Fig.13. Decomposition of $K^*\overline{K}$ and $\overline{K}^*K$ waves to G-parity eigenstates, $J^{PG}M^\eta$.

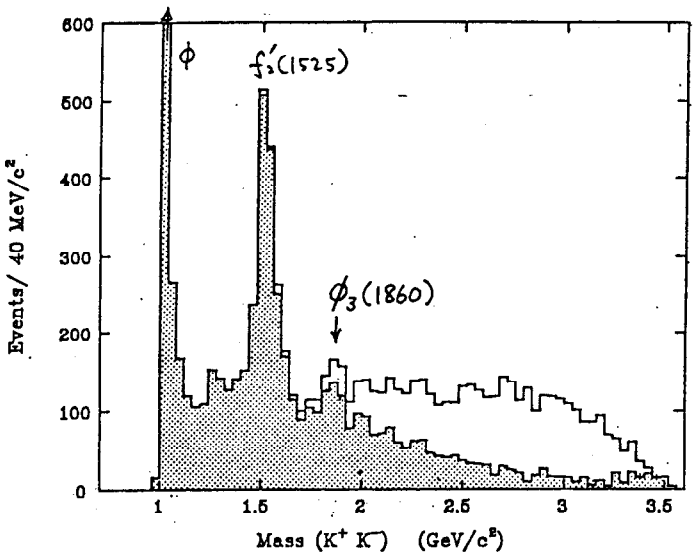

Fig. 14. K^+K^- raw data mass spectrum.

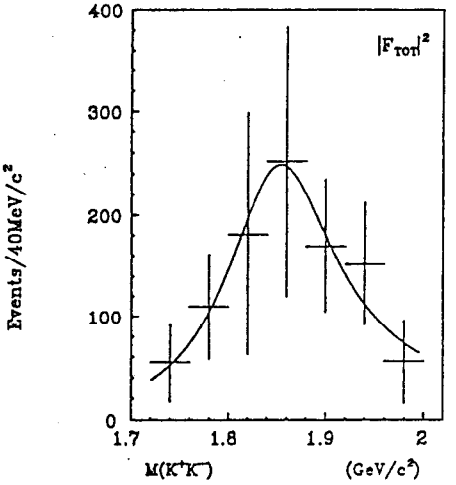

Fig. 16. Modulus of the F-wave amplitude in the $\phi_3(1860)$ region.

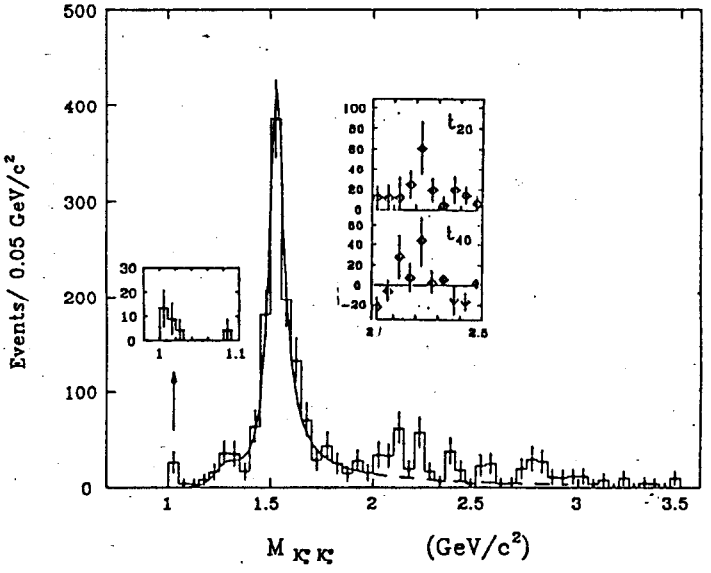

Fig. 15. Acceptance corrected mass spectrum of $K^0_sK^0_s$.

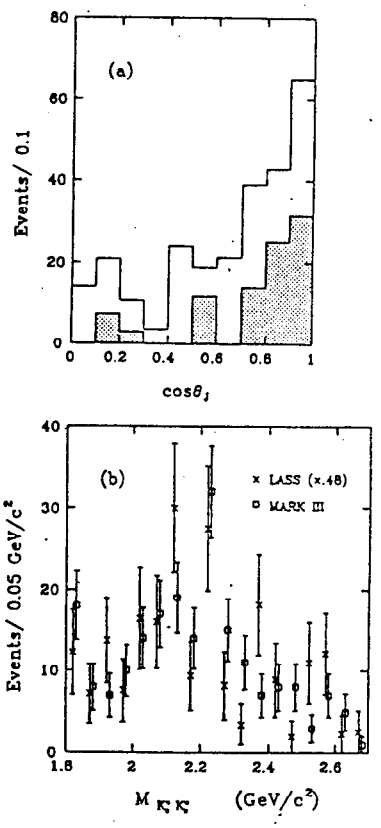

Fig. 17. (a) $cos\theta_J$ distrubution for $2.0 < M_{K^0_sK^0_s} < 2.4$ GeV/c^2 (open histogram), and for $2.15 < M_{K^0_sK^0_s} < 2.3$ GeV/c^2 (shaded histogram).
(b) Comparison of LASS and MARKIII data in $X(2200)$ [ξ] region.

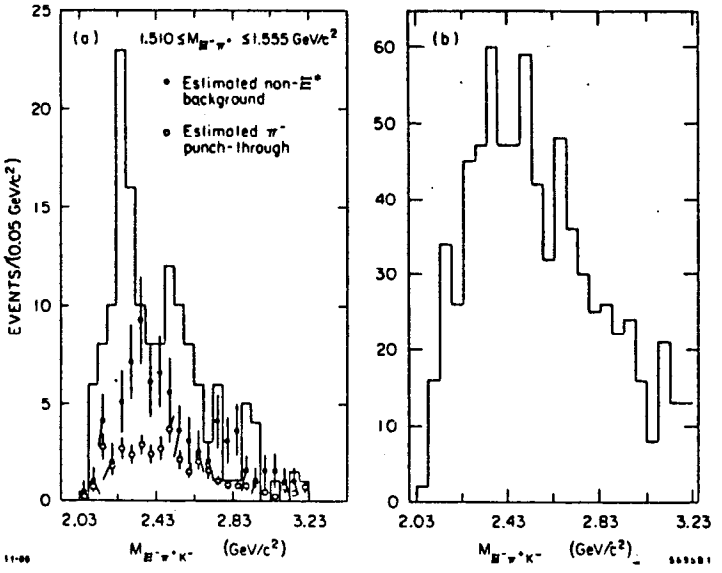

Fig. 18. (a) $\Xi^-\pi^+K^-$ mass spectrum requiring $1.510 \leq M_{\Xi^-\pi^+} \leq 1.555$ GeV/c². (b) $\Xi^-\pi^+K^-$ mass distribution when a positively identified π^- is taken as a "K^-". No fake peak around 2.26 GeV/c² is observed.

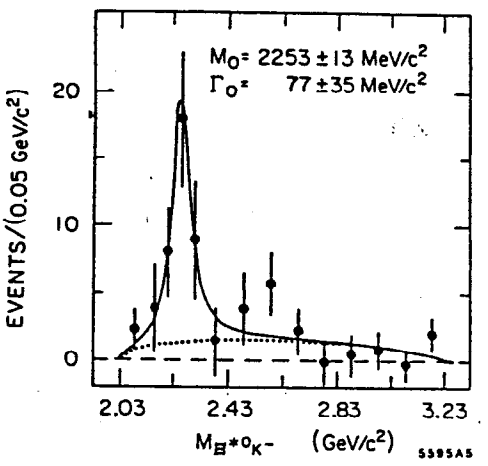

Fig. 19. Background subtracted $\Xi^{*0}K^-$ mass spectrum.

The solid curve represents a Breit-Wigner fit to the Ω^{*-} candidate with simple background form.

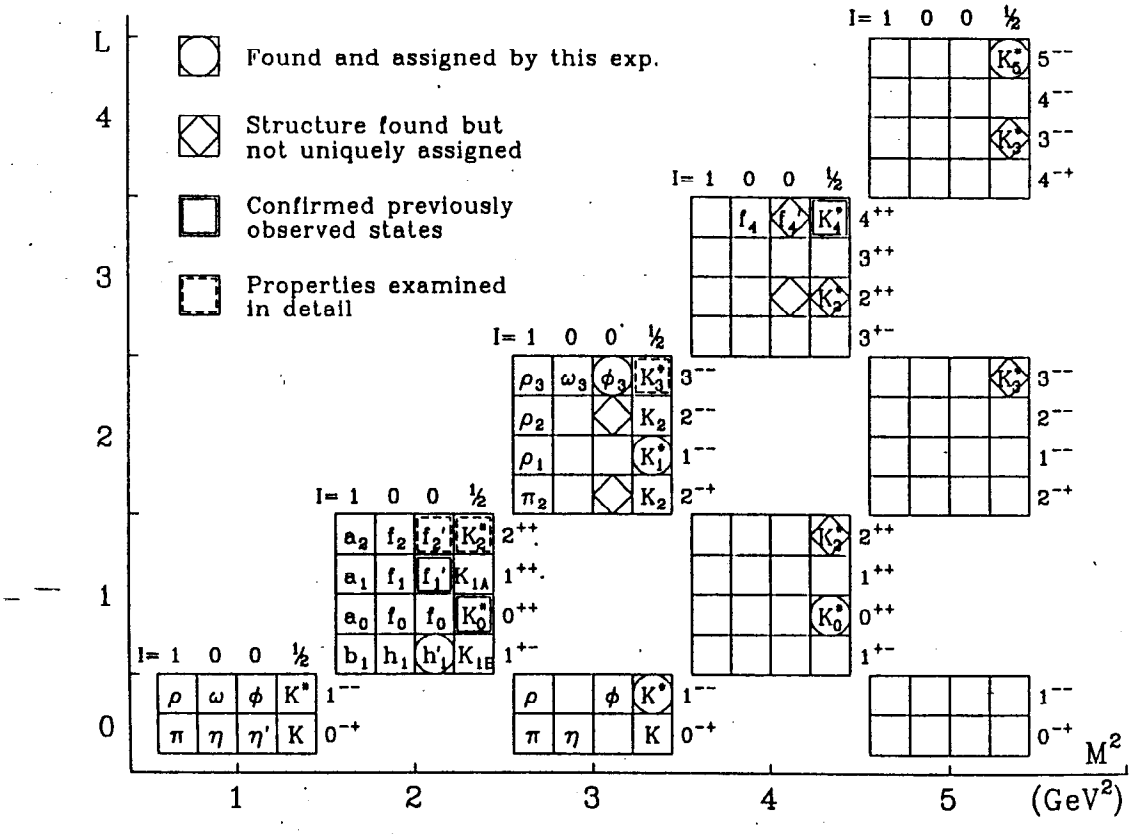

Fig. 20. Summary of mesonic states observed in this experiment.